frontiers
in Materials

Improvement of Flame Retardancy of Polyurethane Foam Using DOPO-Immobilized Silica Aerogel

Xin'guo Zheng[1,2], Quanxiao Dong[2]*, Xi Wang[2], Peiyun Yu[2], Weimin Wang[1], Jinyong Zhang[1] and Lin Ren[1]

[1]College of Materials Science and Engineering, Wuhan University of Technology, Wuhan, China, [2]Railway Engineering Research Institute, China Academy of Railway Sciences Corporation Limited, Beijing, China

In this work, silica aerogel was modified by 9,10-dihydro-9-oxa-10-phosphaphenanthrene-1-oxide (DOPO). Then DOPO-immobilized silica aerogel nanoparticles were used as a flame retardant to prepare flame-retardant polyurethane foams. Microscale combustion calorimeter and cone calorimeter tests were employed to evaluate the flame retardancy of polyurethane foams. It was found that both the heat release rate and the total heat release of the composites were reduced with the incorporation of DOPO immobilized silica aerogel. It is speculated that the DOPO-immobilized silica aerogel nanoparticles can inhibit the degradation of polyurethane and catalyze the formation of carbonaceous carbon on the surface.

Keywords: polyurethane, flame retardancy, DOPO, silica aerogel, mechanism

INTRODUCTION

Polyurethanes are widely applied in automobiles, furniture, coatings, adhesives, and so on (Singh et al., 2009; Xie et al., 2019). Among them, polyurethane foam (PUF) is an excellent insulation material, owing to its low thermal conductivity and outstanding mechanical properties (Liang et al., 2012; Neisius et al., 2012). In recent decades, with people's attention on energy conservation and environmental protection, PUF has been widely used in the field of construction. Unfortunately, it is still a challenge to address the flammability problem of PUF. The oxygen index of PUF is only about 19%, which makes it is easy to be ignited (Xi et al., 2016).

The design purpose of flame retardants is to prevent materials from catching fire and minimize the rate of flame spread (Green et al., 1996; König et al., 2011). In order to stop or delay the combustion process, flame retardants can be incorporated into the PUF system (Liu et al., 2017; Wei et al., 2018). The purpose of using flame retardants is to reduce the inherent fire risk of polyurethane by reducing the burning rate and the spread of flame in the presence of fire. Currently, two types of flame retardants (additive and reactive agents) could be used to prepare flame-retardant PU foams (Modesti et al., 2002; Gaan et al., 2015; Xu et al., 2015; Chen et al., 2018; Chen et al., 2019; Jia et al., 2019). The additive flame retardant is suspended in the foam matrix during the preparation process to provide flame retardancy. However, they show the possibility of chronological migration affecting fire resistance (Zhang et al., 2020; Xue et al., 2020). At the same time, due to the lack of strong covalent adhesion of PUF, the flame retardant deteriorates due to migration during the combustion process (Chai et al., 2019; Li et al., 2019; Yu et al., 2021; Zhang et al., 2021).

Generally speaking, common halogen flame retardants could improve the flame retardancy of polymeric materials, but toxic gases could be released during the combustion process (Papa et al., 1972; Salthammer et al., 2003). Therefore, it is necessary to promote the development of halogen-free

flame retardants (Guo et al., 2020; He et al., 2020). Recently, halogen-free flame retardants have been developed and applied in the preparation of polyurethane (Zhu et al., 2014; Ding et al., 2016; Jiao et al., 2019; Sykam et al., 2019; Xia et al., 2020). Among them, phosphorus-containing flame retardants, especially 9,10-dihydro-9-oxa-10-phosphaphenanthrene-10-oxide (DOPO) and its derivatives, have attracted much attention (Huo et al., 2020; Huo et al., 2021). 9,10-Dihydro-9-oxa-10-phenanthrene-10-oxide (DOPO) and its derivatives were used to improve their use as flame retardants, as these have higher thermal stability, excellent flame retardancy, and low toxicity (Ma et al., 2020; Zhi et al., 2020).

Silica aerogel (SA) was developed by Kistler (Kistler., 1931). It is an ultralight porous material with a spatial reticular porous structure consists of cross-linked silicone particles. SA has excellent properties, such as high specific surface ($500–1,200\ m^2{\cdot}g^{-1}$), high porosity (80–99.8%), low density ($0.003–0.5\ g{\cdot}cm^{-3}$), low thermal conductivity ($0.005–0.1\ W{\cdot}m^{-1}{\cdot}K^{-1}$). As a unique porous material, SA is not easy to be decomposed at high temperatures due to its good flame retardancy (Yuan et al., 2016; Yu et al., 2017). As a flame retardant, it could form a silica aerogel coating to promote the formation of the char layer, increasing the strength of the char layer during combustion of polymer materials, also improving the flame retardant performance of the polymer. However, aerogels are easily tended to generate agglomerate in the polymer matrix, which hinders their application in flame retardancy.

The surface modification of nano-silica is usually achieved by grafting polymer chains to obtain a better dispersion effect. In recent years, more and more studies report the synthesis of additive-type nanoparticles by grafting functional molecules on the surface of the nanoparticles (Bartholome et al., 2003; Tsubokawa et al., 2007; Vejayakumaran et al., 2008; Zhao et al., 2012). Surface grafting can not only inhibit the migration of flame retardants but also improve the dispersibility of the nanoparticles in the matrix. The coupling agent method is a common way to graft functional molecules to the surface of nanoparticles. Silane coupling agents are usually expressed as $RSiX_3$, where -X can be hydrolyzed to form silanol and react with hydroxyl on the filler surface, and -R can be grafted with other functional compounds. Therefore, nano silica can be functionalized by using a silane coupling agent (Radhakrishnan et al., 2006). In the present work, bifunctional coupling agents 3-methacryloxy-propyltrimethoxy-silane (WD70) were used to introduce C=C groups onto the surface of silica aerogel nanoparticles. Then, DOPO was immobilized on the surface of SiO_2 nanoparticles through the reaction with C=C bonds.

In this work, DOPO immobilized silica aerogel (SA-g-DOPO) was synthesized successfully by the combination of the nano silica aerogel (SA), silane coupling agent, and DOPO through a two-step process. The synthesized nanoparticles were used as a flame-retardant additive for polyurethane. A thermo gravimetric analyzer (TGA), scanning electron microscope (SEM), cone calorimeter test (CCT), and micro-scale combustion calorimeter (MCC) were used to study the thermal and flame-retardant properties of PUF.

MATERIALS AND METHODS

Materials

SiO_2 was provided by Evonik Degussa-Hüls. 3-Methacryloxypropyltrimethoxy-silane (WD70) was supplied by Energy Chemical. 9,10-Dihydro-9-oxa-10-phosphaphenanthrene-10-oxide (DOPO) was provided by Jiangsu Huihongjinpu Chemical Co. Ltd., Jiangsu, China. Methylbenzene, triethylamine, and absolute ethyl alcohol were purchased from Beijing Chemical Reagent Co., Beijing, China. Polyol compositions (FR715) were obtained from Shandong Ogasen New Material Co. Ltd., Shandong, China. Polyaryl polyisocyanate (WANNATE PM200) was supplied by Wanhua Chemical Group Co. Ltd., Shandong, China. Deionized water was obtained from our laboratory.

Synthesis of Hydroxy Activated Silica Aerogel (SA-OH)

The hydroxy activated silica aerogel defined as SA-OH was synthesized according to the following steps. First, 5.0 g silica aerogel (SA) was processed at 300°C in the muffle furnace for 30 min, and then it was activated by piranha solution (H_2SO_4/H_2O_2 7:3, volume ratio) in an oil bath at 90°C for 24 h. Then, dilute the mixture with deionized water and centrifuge (10,000 rpm, 10 min). Finally, after two centrifugation/re-dispersion cycles, the mixture was washed with absolute ethanol repeatedly. The obtained SA-OH was all white solid powders. The synthetic route of SA-OH is shown in **Figure 1**.

Preparation of DOPO-Immobilized Silica Aerogel (SA-g-DOPO)

At first, DOPO (5.25 g, dissolved in 120 ml of anhydrous toluene) was added in a 500 ml three-necked round bottom flask equipped with a nitrogen inlet and a reflux condenser. Then, WD70 (5.0 g, dissolved in 60 ml of anhydrous toluene) was added into the above-mentioned solution and stirred for over 0.5 h. Next, triethylamine (0.5 g) was added dropwise in three portions. The mixture was under reflux with continuous stirring under nitrogen atmosphere at 110°C for 24 h. Afterwards, 5.0 g SA-OH and 180 ml toluene were added to the mixture solution and reacted at the same condition for another 24 h. Last, the product was filtered immediately and washed with anhydrous ethanol (200 ml) five times before being dried at 110°C to achieve a constant weight. The reaction process is illustrated in **Figure 2**.

As shown in **Figure 1**, after treating with piranha solution, the aerogel had higher hydroxyl content on the surface. As shown in **Figure 2**, as DOPO has a phosphorous heterocyclic structure and P has lone pair electrons, it is prone to nucleophilic addition. In the meanwhile, the C=C and ester group of WD70 can form a conjugate system. This kind of conjugate system lowered the Π electron density of the C=C and made nucleophiles easily close to the carbon atoms. Thus, under the condition of triethylamine as a catalyst, DOPO could react with WD70. Subsequently, the siloxy group of WD70 hydrolyzed into silanol and reacted with the hydroxyl on the surface of the activated aerogel, which introduced DOPO to the surface of the aerogel.
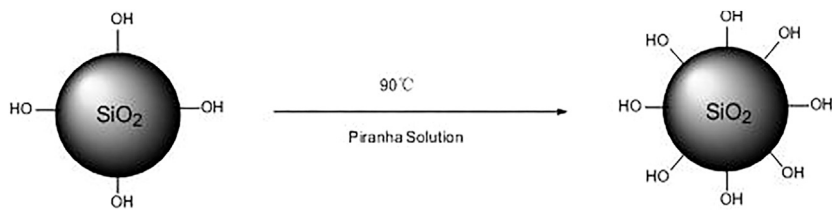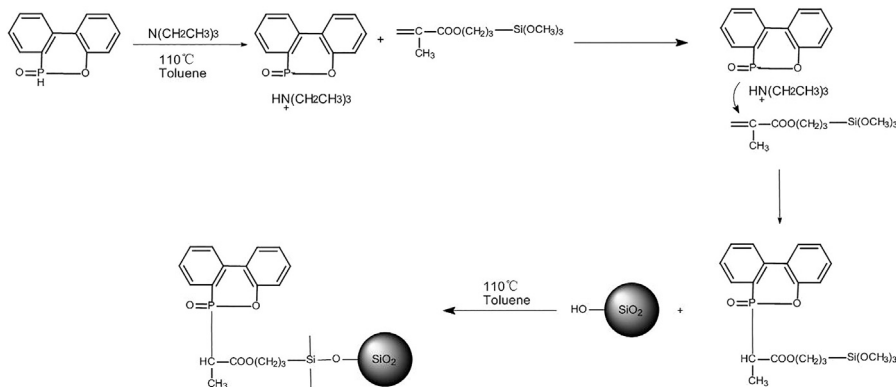
FIGURE 1 | Preparation of SA-OH

FIGURE 2 | The synthetic route of SA-g-DOPO.

TABLE 1 | PUF compounds and the compositions.

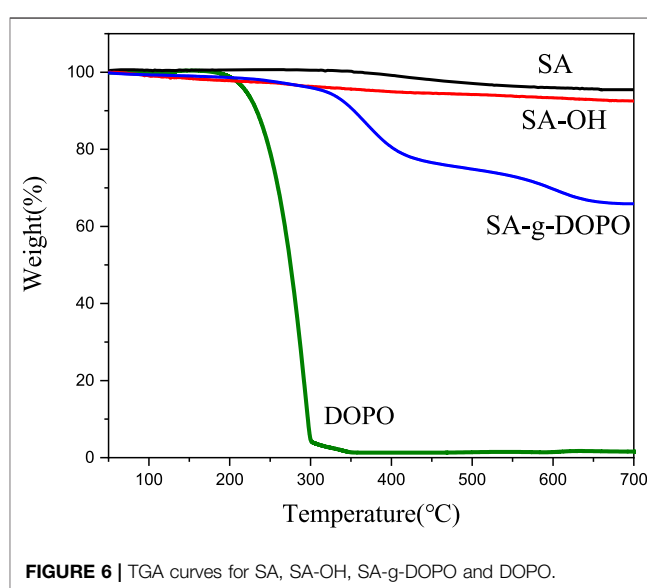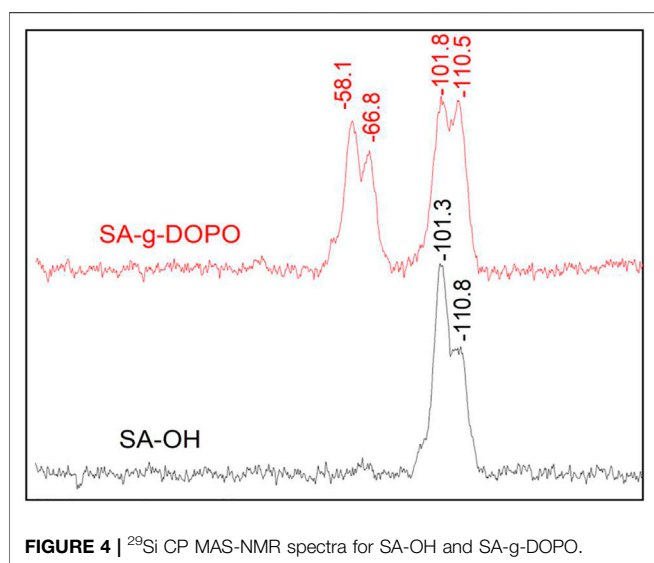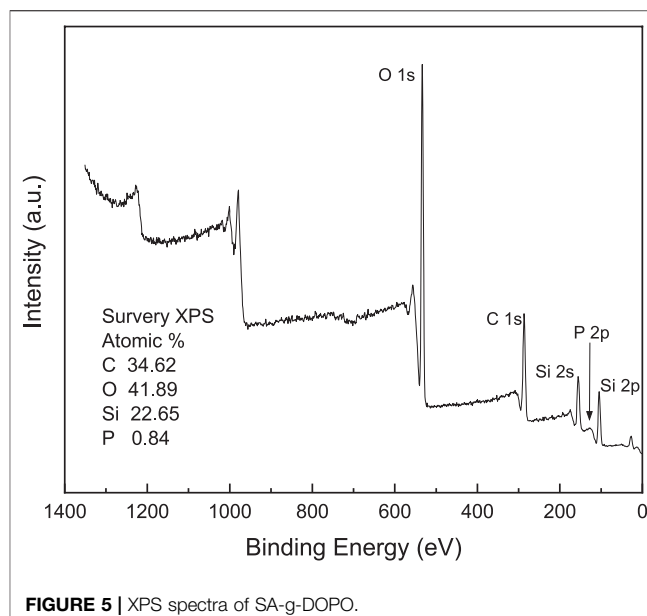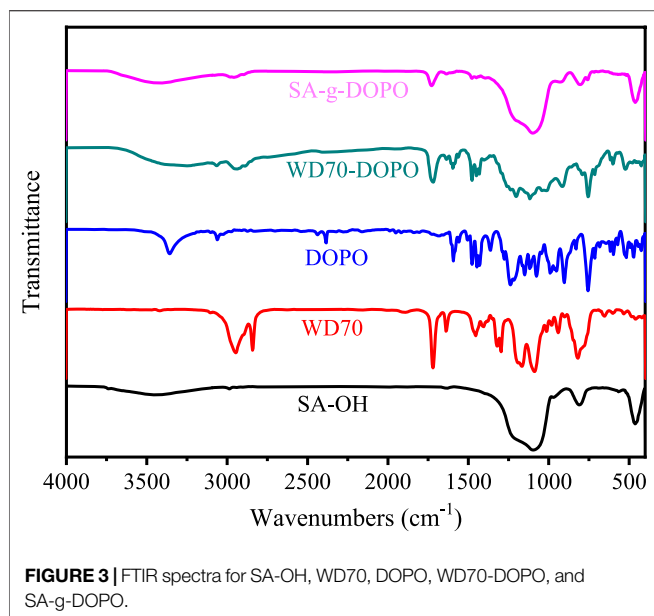| Samples	Type of additives	Content of additives (wt%)
PUF	-	-
PUF/SA-OH	SA-OH	5
PUF/SA-g-DOPO	SA-g-DOPO	6.5
PUF/SA-OH/DOPO	SA-OH + DOPO	5 + 1.5
PUF/DOPO	DOPO	1.5

Preparation of PUF

The pure PUF, SA-OH containing PUF, and SA-g-DOPO containing PUF were produced by the one-pot method. Briefly, polyol alcohol, isocyanate (weight ratio = 1:0.47), distilled water, catalyst, and flame retardant were incorporated into a 1 L plastic cup and thoroughly mixed by mechanical stirring under high speed for 10 s. The mixture was immediately poured into an opened mold. The formulation of PUF is shown in **Table 1**. The abbreviations of the five PUF are PUF, PUF/SA-OH, PUF/SA-g-DOPO,PUF/SA-OH/DOPO, and PUF/DOPO.

Measurements

The molecular structures of SA-OH, WD70, DOPO, WD70-DOPO, and SA-g-DOPO were characterized by Fourier

transform infrared (FTIR). The FTIR spectra of the samples were recorded on a Nicolet 6,700 spectrometer in the range of 400–4,000 cm^{-1} at a scan number of 32 and a resolution of 4 cm^{-1}. The thermal stability of the specimen was tested using a Q600 SDT (TA, United States). Each specimen was heated from room temperature to 800°C under air atmosphere with a flow rate of 20 ml min^{-1} and a heating rate of 10°C min^{-1} in an alumina crucible. Solid ^{29}Si MAS-NMR studies were performed via a Bruker Avanve III 400 NMR pectrometer with a magic angle spinning technique. Magic angle spinning was performed at 79.3 MHz with a 5 kHz spin rate for ^{29}Si study. Cone calorimeter test (CCT) was performed using an FTT2000 cone calorimeter instrument according to ISO 5660-1. Three samples were used in this test. Each sample of 100 mm × 100 mm × 20 mm (length × width × thickness) was wrapped in aluminum foil and exposed. A scanning electron microscope (SEM) was used to examine the morphology of the char residue obtained after cone calorimeter test using a Hitachi S-4800 scanning electron microscope at an accelerating voltage of 15 kV. The residual surfaces were coated with a thin gold layer. Microscale combustion calorimetry (MCC) was carried out using an FAA Micro calorimeter (FAA Fire testing technology, East Grinstead, United Kingdom) operated at 1°C s^{-1}–750°C in the pyrolysis zone according to ASTM D7309 method A. Three specimens were used in this characterization. The combustion zone was set at 900°C. Oxygen and nitrogen flow rates were set at 20 and 80 ml min^{-1}, respectively.

FIGURE 3 | FTIR spectra for SA-OH, WD70, DOPO, WD70-DOPO, and SA-g-DOPO.

FIGURE 5 | XPS spectra of SA-g-DOPO.

FIGURE 4 | ^{29}Si CP MAS-NMR spectra for SA-OH and SA-g-DOPO.

FIGURE 6 | TGA curves for SA, SA-OH, SA-g-DOPO and DOPO.

RESULTS AND DISCUSSION

Characterization of SA-g-DOPO

The chemical structures of SA-OH, WD70, DOPO, and synthesized WD70-DOPO and SA-g-DOPO were characterized by FTIR. As shown in **Figure 3**, the peak at 2,385 cm^{-1} corresponds to the stretching vibration of the P-H bond. It can be found from the spectrum of SA-OH that the characteristic peak of P-O-H stretching vibration of silanol hydroxyls and adsorbed water appears at 3,434 cm^{-1}. For WD70, the absorption peak at 1710 cm^{-1} is attributed to the tensile vibration of C=O bond. The asymmetrical and symmetrical stretching absorption bands for $-CH_3$ and $-CH_2-$ groups were confirmed by the peaks at 2,979 cm^{-1} and

2,864 cm^{-1}. The peak at 1710 cm^{-1} became weak after DOPO was introduced to WD70, which showed that DOPO reacted with WD70. The above analysis confirmed the structure of WD70-DOPO. For SA-g-DOPO, it can be seen that the bands at 1710 cm^{-1} were the same as with WD70-DOPO. As shown in the Solid ^{29}Si MAS-NMR spectrum (**Figure 4**), two additional peaks were found at −58.1 and −66.8 ppm, which represented bidental and monodental structures, respectively. The newly observed peaks proved that one or two methoxy groups of silane coupling agents reacted with SA-OH. X-ray photoelectron spectroscopy (XPS) was used to characterize the surface P% elemental of the SA-g-DOPO nanoparticles. As shown in **Figure 5**, 0.84% P was detected on the surface of the
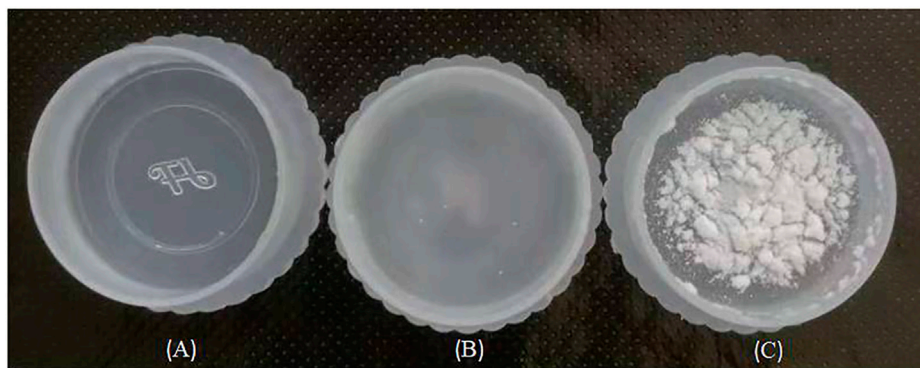
FIGURE 7 | Picture of SA-OH and SA-g-DOPO in the water.

modified nanoparticles. All the results confirmed the successful addition reaction between DOPO and the surface of SA-OH.

Thermogravimetric Analysis of SA-g-DOPO

As shown in **Figure 6**, the initial decomposition temperature of the SA, SA-OH, and synthesized SA-g-DOPO are all higher than 270°C. Compared with DOPO, carbon residue is also significantly improved. As shown in **Figure 6**, the unmodified silica aerogel (SA) had only 4.6 wt% weight loss while the SA-OH had 7.5 wt% weight loss at the end temperature (700°C). This is mainly because the content of hydroxyl on the surface of silica aerogel has increased significantly after the surface activation of silica aerogel. The weight loss at the end temperature was 34.2 wt% and 0.3 wt% for SA-g-DOPO and DOPO, respectively. The results show that the amount of immobilized DOPO on silica aerogel surface was 33.9 wt%, while the grafting amount of DOPO derivatives in the traditional method was less than 10 wt%. Compared with the common DOPO flame retardant intermediates, SA-g-DOPO has higher thermal stability and charring properties.

Surface Wettability of DOPO-Immobilized Silica Aerogel

The surface wettability of DOPO-immobilized silica aerogel and SA-OH samples is shown in **Figure 7**. It can be observed that SA-OH was completely dissolved while SA-g-DOPO floated in water. According to **Figure 7**, the surface wettability was relatively affected by the molecular structure of the silica aerogel. In this study, such a result can be ascribed to the surface of SA-OH has a lot of hydroxyl groups and SA-OH is highly hydrophilic. On the other hand, the amount of hydroxyl decreased and the organic groups increased after DOPO had been immobilized to the surface of SA-OH, which introduced an improvement in the hydrophobicity of SA-g-DOPO.

MCC Results of PUF Composites

The combustion performances of PUF, PUF/SA-OH, PUF/SA-g-DOPO, PUF/SA-OH/DOPO, and PUF/DOPO were characterized by micro combustion calorimeter (MCC). As shown in **Figure 8** and **Table 2**, the PHRR and THR of PUF were 415 W g^{-1} and 24.0 kJ g^{-1}, respectively. After SA-OH was added, the PHRR of the composites decreased to 416 W g^{-1} (decreased by 10.4%) and the THR decreased
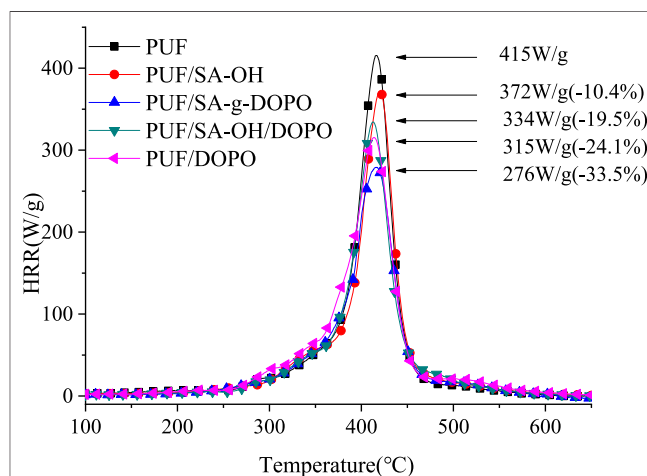

FIGURE 8 | MCC curves for PUF composites.

to 22.7 kJ g^{-1} (decreased by 5.4%). It is speculated that SA-OH could catalyze the formation of carbon from PUF pyrolysis products. The stable char layer formed could inhibit the exchange of materials and energy in the combustion area, thus inhibiting the further development of combustion (Wang et al., 2011; Dong et al., 2012; Jiang et al., 2016). When DOPO was added to PUF, the PHRR of the material decreased to 315 W g^{-1}, (decreased by 24.1%) and THR decreased to 23.6 kJ g^{-1} (decreased by 1.7%). It means that DOPO could only reduce the heat release rate of the PUF, and it had little impact on the total heat release. The reason was that PO could be released from DOPO under the effect of heat, thus inhibiting the degradation of polyurethane and improving the flame retardance of the materials (Yang et al., 2019; Huo et al., 2019). After SA-OH and DOPO were blended physically and added to PUF, the PHRR of the material decreased to 334 W g^{-1} (decreases by 19.5%), which is lower than that of SA-OH, but higher than that of DOPO added alone. In addition, the THR decreased to 21.7 kJ g^{-1} (decreased by 9.6%), lower than SA-OH or DOPO added separately. With the incorporation SA-g-DOPO into PUF, the PHRR of the composite significantly decreased to 276 W g^{-1} (decreased by 33.5%) and THR decreased to 19.9 kJ g^{-1} (decreased by 17.1%). That is because SA-g-DOPO

TABLE 2 | MCC results of PUF composites.

Sample	PHRR (W·g^{-1})	T$_{PHRR}$ (°C)	THR (kJ·g^{-1})	HRC (J g^{-1}·K^{-1})
PUF	415	413	24.0	427
PUF/SA-OH	372	416	22.7	380
PUF/SA-g-DOPO	276	392	19.9	283
PUF/SA-OH/DOPO	334	410	21.7	344
PUF/DOPO	315	408	23.6	322

TABLE 3 | CCT results of PUF composites.

Sample	PkHRR (kW.m^{-2})	TPkHRR (s)	AvHRR (kW.m^{-2})	CY (%)
PUF	782.8	120	227.9	0
PUF/SA-OH	383.3	400	184.5	11.20
PUF/SA -g-DOPO	345.1	140	175.7	11.02
PUF/SA-OH/DOPO	354.3	535	180.8	15.12
PUF/DOPO	659.8	140	180.6	4.92

PkHRR, Peak Heat Release Rate; TPkHRR, Time to Peak Heat Release Rate; AvHRR, Average Heat Release Rate; CY, Char Yield.
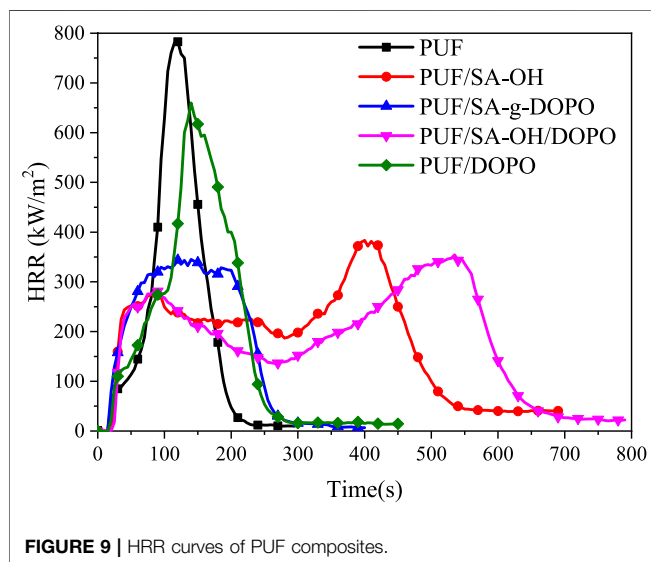
FIGURE 9 | HRR curves of PUF composites.

could promote the formation of the char layer and inhibited the further combustion of the material during the combustion process. On the other hand, the PO released from DOPO which immobilized on the surface of silica aerogel inhibited the degradation of the material, thus making up for the defects of the physical blending of SA-OH and DOPO.

Combustion Performance of PUF Composites

A cone calorimeter test (CCT) is a bench-scale instrument that is widely used to study the fire hazards of materials (Xie et al., 2017; Gallina et al., 1998). The test could give out comprehensive fire and smoke parameters to predict the probable performances of the material in an actual fire, which includes peak heat release rate (PkHRR), time to peak heat release rate (TPkHRR), average heat release rate (AvHRR), and char yield (CY). These parameters are summarized in **Table 3**. It is indicated that the peak heat release rate was decreased after the incorporation of SA-g-DOPO. As shown in **Figure 9**, it is obvious that after adding a flame retardant, PkHRR values became lower than those of pure PUF. Furthermore, pristine PUF was easy to be ignited and burned out rapidly after ignition. Therefore, the highest values of PHRR and THR of pristine PUF were obtained with few residues left. Compared with pristine PUF, with the incorporation of SA-g-DOPO into PUFs, the PkHRR values and AvHRR values decreased to 345.1 kW m^{-2} (−51%) and 175.7 kW·m^{-2} (−22.9%), respectively. This phenomenon is due to the increase in the density of PUF/SA-g-DOPO, and is also related to the enhancement of the gas phase flame retardant effect of DOPO. In addition, as the content of SA-g-DOPO increased, the residues also increased significantly.

When SA-OH and DOPO were incorporated into PUF together, the curve was basically consistent with that of adding SA-OH. The maximum heat release rate was reduced. At the same time, the existence of DOPO would improve the stability of the char layer to some extent and prolong its existence time. After adding SA-g-DOPO to PUF, the PkHRR decreased to 345.1 kW m^{-2} (−55.9%). An analysis of this was that SA-g-DOPO induced the generating of char layer during the process of burning, which reduced the amount of the produced heat return to the matrix. In addition, SA-g-DOPO may affect the degradation of the material, which further increased the stability of the char layer than the physical blending way.

Char Residue Analysis After Cone Calorimeter Tests

The residue morphology after cone calorimetric tests was investigated. As shown in **Figure 10A**, there is almost no

FIGURE 10 | PUF char layer after combustion (A: PUF, B: PUF/SA-g-DOPO).
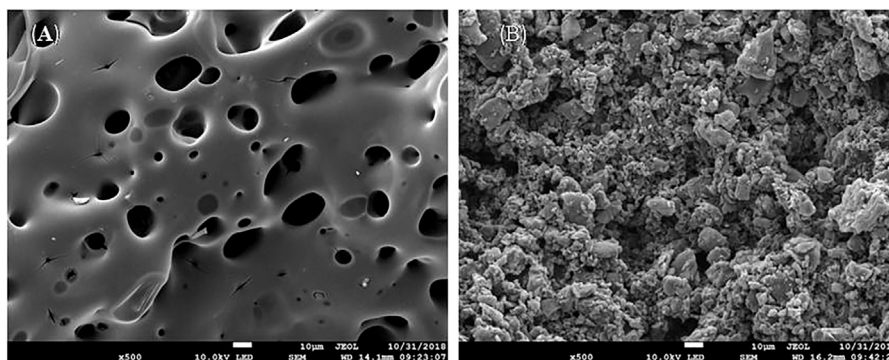

FIGURE 11 | SEM images of char residues of PUFs (A: PUF, B: PUF/SA-g-DOPO).

residual char left in the pure PUF. It can be seen that a small amount of the residual char with an obviously broken structure on the surface. The char can not effectively prevent the inner matrix from further combustion. As for PUF/SA-g-DOPO (**Figure 10B**), the charred layer has a more rigid and compact surface. This kind of char could act as a shield to prevent heat, air, and pyrolysis product transfer. It is found that the charred layer becomes more continuous and integrated by the incorporation of SA-g-DOPO into PUF. This kind of char layer could effectively prevent the release of combustible volatiles and the thermal feedback of the flame. Thus, the flame retardancy property could be improved.

SEM micrographs of the surface from the pure PUF and PUF/SA-g-DOPO residual chars are shown in **Figure 11**. The residual char of PUF is loose and porous (**Figure 11**), which is a poor protective layer. Compared with pure PUF, a compact char layer was generated for PUF/SA-g-DOPO. It is indicated that the expanded residual coke structure can form a protective layer to prevent heat transfer, oxygen diffusion.
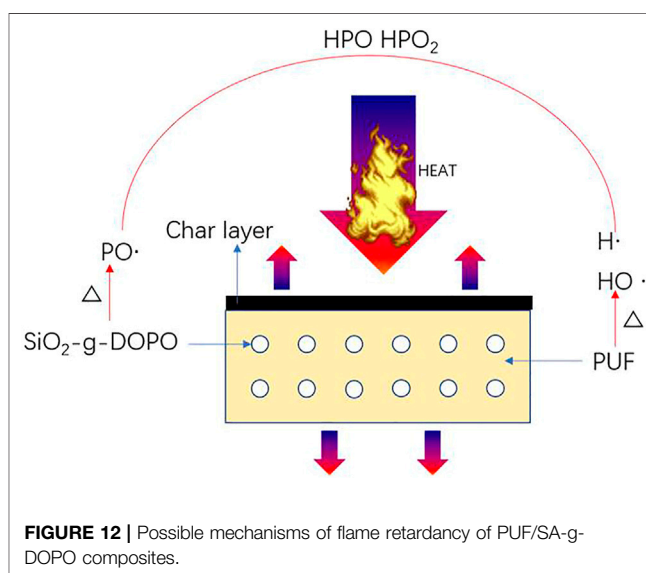

FIGURE 12 | Possible mechanisms of flame retardancy of PUF/SA-g-DOPO composites.

Flame Retardant Mechanism of PUF Composites

Based on the abovementioned results, the flame-retardant mechanism of SA-g-DOPO in polyurethane foam is proposed (**Figure 12**). Firstly, during the combustion of the foams, the phosphorus-containing polyurethane decomposed to isocyanates and alcohols. By increasing the temperature, SA-g-DOPO would generate polyphosphoric acids, which can capture the H and OH·. The generated polyphosphoric acids could promote the formation of a thermally stable char. The compact char layer could act as a good barrier effect. The generated char could effectively prevent decomposition of polyurethane foam. The mass loss rate could be delayed. Thus, the release of volatile products could be suppressed. Secondly, the char layer prevents the further degradation of volatile products, and flame retardancy property was improved.

CONCLUSION

The flame retardancy of PUF/SA-g-DOPO composites was increased with the incorporation of SA-g-DOPO. Specifically, TGA results showed that the content of hydroxyl on the surface of aerogels increased from 4.8 wt% to 7.5 wt%. And the amount of DOPO derivatives that are grafted can be increased to 34.1 wt%. MCC results showed that the PHRR and THR decreased by 33.5 and 17.1% respectively after SA-g-DOPO incorporated into PUF. The calorimetric results showed that with the incorporation of SA-g-DOPO into PUF, the PkHRR of composites decreased from $782.8\,\mathrm{kW\,m^{-2}}$–$345.1\,\mathrm{kW\,m^{-2}}$, with a decrease of 55.9%. The combination of SA and DOPO effectively could delay the material degradation products and heat transfer of PUF in the combustion process. The thermal stability and flame resistance of PUF was improved. With the incorporation of SA-g-DOPO, the fire risk of PUF was reduced.

ADDITIONAL REQUIREMENTS

For additional requirements for specific article types and further information please refer to Author Guidelines.

DATA AVAILABILITY STATEMENT

The original contributions presented in the study are included in the article/Supplementary Material, further inquiries can be directed to the corresponding author.

AUTHOR CONTRIBUTIONS

Conceptualization, QD and XZ; Data curation, XW and PY; Formal analysis, LR; Investigation, WW and JZ; Methodology, QD; Supervision, WW.

FUNDING

REFERENCES

Bartholome, C., Beyou, E., Bourgeat-Lami, E., Chaumont, P., and Zydowicz, N. (2003). Nitroxide-Mediated Polymerizations from Silica Nanoparticle Surfaces: "Graft from" Polymerization of Styrene Using a Triethoxysilyl-Terminated Alkoxyamine Initiator. *Macromolecules* 36, 7946–7952. doi:10.1021/ma034491u

Chai, H., Duan, Q., Jiang, L., and Sun, J. (2019). Effect of Inorganic Additive Flame Retardant on Fire hazard of Polyurethane Exterior Insulation Material. *J. Therm. Anal. Calorim.* 135, 2857–2868. doi:10.1007/s10973-018-7797-3

Chen, Y., Li, L., Qi, X., and Qian, L. (2019). The Pyrolysis Behaviors of Phosphorus-Containing Organosilicon Compound Modified APP with Different Polyether Segments and Their Flame Retardant Mechanism in Polyurethane Foam. *Composites B: Eng.* 173, 106784–106791. doi:10.1016/j.compositesb.2019.04.045

Chen, Y., Li, L., and Qian, L. (2018). The Pyrolysis Behaviors of Phosphorus-Containing Organosilicon Compound Modified Ammonium Polyphosphate with Different Phosphorus-Containing Groups, and Their Different Flame-Retardant Mechanisms in Polyurethane Foam. *RSC Adv.* 8, 27470–27480. doi:10.1039/C8RA04439B10.1039/c8ra04439b

Ding, H., Xia, C., Wang, J., Wang, C., and Chu, F. (2016). Inherently Flame-Retardant Flexible Bio-Based Polyurethane Sealant with Phosphorus and Nitrogen-Containing Polyurethane Prepolymer. *J. Mater. Sci.* 51, 5008–5018. doi:10.1007/s10853-016-9805-y

Dong, Q., Ding, Y., Wen, B., Wang, F., Dong, H., Zhang, S., et al. (2012). Improvement of Thermal Stability of Polypropylene Using DOPO-Immobilized Silica Nanoparticles. *Colloid Polym. Sci.* 290, 1371–1380. doi:10.1007/s00396-012-2631-0

Gaan, S., Liang, S., Mispreuve, H., Perler, H., Naescher, R., and Neisius, M. (2015). Flame Retardant Flexible Polyurethane Foams from Novel DOPO-Phosphonamidate Additives. *Polym. Degrad. Stab.* 113, 180–188. doi:10.1016/j.polymdegradstab.2015.01.007

Gallina, G., Bravin, E., Badalucco, C., Audisio, G., Armanini, M., De Chirico, A., et al. (1998). Application of Cone Calorimeter for the Assessment of Class of Flame Retardants for Polypropylene. *Fire Mater.* 22, 15–18. doi:10.1002/(sici)1099-1018(199801/02)22:1<15::aid-fam626>3.0.co;2-3

Green, J. (1996). Mechanisms for Flame Retardancy and Smoke Suppression -A Review. *J. Fire Sci.* 14, 426–442. doi:10.1177/073490419601400602

Guo, K.-Y., Wu, Q., Mao, M., Chen, H., Zhang, G.-D., Zhao, L., et al. (2020). Water-based Hybrid Coatings toward Mechanically Flexible, Super-hydrophobic and Flame-Retardant Polyurethane Foam Nanocomposites with High-Efficiency and Reliable Fire Alarm Response. *Composites Part B: Eng.*, 193, 108017. doi:10.1016/j.compositesb.2020.108017

He, W., Song, P., Yu, B., Fang, Z., and Wang, H. (2020). Flame Retardant Polymeric Nanocomposites through the Combination of Nanomaterials and Conventional Flame Retardants. *Prog. Mater. Sci.* 114, 100687. doi:10.1016/j.pmatsci.2020.100687

Huo, S., Liu, Z., and Wang, J. (2019). Thermal Properties and Flame Retardancy of an Intumescent Flame-Retarded Epoxy System Containing Phosphaphenanthrene, Triazine-Trione and Piperidine. *J. Therm. Anal. Calorim.* 139, 1099–1110. doi:10.1007/s10973-019-08467-3

Huo, S., Song, P., Yu, B., Ran, S., Chevali, V. S., Liu, L., et al. (2021). Phosphorus-containing Flame Retardant Epoxy Thermosets: Recent Advances and Future Perspectives. *Prog. Polym. Sci.* 114, 101366. doi:10.1016/j.progpolymsci.2021.101366

Huo, S., Yang, S., Wang, J., Cheng, J., Zhang, Q., Hu, Y., et al. (2020). A Liquid Phosphorus-Containing Imidazole Derivative as Flame-Retardant Curing Agent for Epoxy Resin with Enhanced thermal Latency, Mechanical, and Flame-Retardant Performances. *J. Hazard. Mater.* 386, 121984. doi:10.1016/j.jhazmat.2019.121984

Jia, D., Guo, X., He, J., and Yang, R. (2019). An Anti-melt Dripping, High Char Yield and Flame-Retardant Polyether Rigid Polyurethane Foam. *Polym. Degrad. Stab.* 167, 189–200. doi:10.1016/j.polymdegradstab.2019.07.007

Jiang, S., Zhu, Y., Hu, Y., Chen, G., Shi, X., and Qian, X. (2016). In Situsynthesis of a Novel Transparent Poly (Methyl Methacrylate) Resin with Markedly Enhanced Flame Retardancy. *Polym. Adv. Technol.* 27, 266–272. doi:10.1002/pat.3631

Jiao, C., Wang, H., Chen, X., and Tang, G. (2019). Flame Retardant and thermal Degradation Properties of Flame Retardant Thermoplastic Polyurethane Based on HGM@[EOOOEMIm][BF4]. *J. Therm. Anal. Calorim.* 135, 3141–3152. doi:10.1007/s10973-018-7505-3

Kistler, S. S. (1931). Coherent Expanded Aerogels and Jellies. *Nature* 127, 741. doi:10.1038/127741a0

König, A., and Kroke, E. (2011). Methyl-DOPO-a New Flame Retardant for Flexible Polyurethane Foam. *Polym. Adv. Technol.* 22, 5–13. doi:10.1002/pat.1728

Li, L., Chen, Y., Wu, X., Xu, B., and Qian, L. (2019). Bi-phase Flame-retardant Effect of Dimethyl Methylphosphonate and Modified Ammonium Polyphosphate on Rigid Polyurethane Foam. *Polym. Adv. Technol.* 30, 2721–2728. doi:10.1002/pat.4702

Liang, S., Neisius, M., Mispreuve, H., Naescher, R., and Gaan, S. (2012). Flame Retardancy and thermal Decomposition of Flexible Polyurethane Foams: Structural Influence of Organophosphorus Compounds. *Polym. Degrad. Stab.* 97, 2428–2440. doi:10.1016/j.polymdegradstab.2012.07.019

Liu, X., Salmeia, K. A., Rentsch, D., Hao, J., and Gaan, S. (2017). Thermal Decomposition and Flammability of Rigid PU Foams Containing Some DOPO Derivatives and Other Phosphorus Compounds. *J. Anal. Appl. Pyrolysis* 124, 219–229. doi:10.1016/j.jaap.2017.02.003

Ma, S., Xiao, Y., Zhou, F., Schartel, B., Chan, Y. Y., Korobeinichev, O. P., et al. (2020). Effects of Novel Phosphorus-Nitrogen-Containing DOPO Derivative Salts on Mechanical Properties, thermal Stability and Flame Retardancy of Flexible Polyurethane Foam. *Polym. Degrad. Stab.* 177, 109160–160. doi:10.1016/j.polymdegradstab.2020.109160

Modesti, M., Lorenzetti, A., Simioni, F., and Camino, G. (2002). Expandable Graphite as an Intumescent Flame Retardant in Polyisocyanurate-Polyurethane Foams. *Polym. Degrad. Stab.* 77, 195–202. doi:10.1016/s0141-3910(02)00034-4

Neisius, N. M., Liang, S., Mispreuve, H., and Gaan, S. (2012). Recent Developments in Flame Retardancy of Flexible Polyurethane Foams. in *Fire and Polymers VI: New Advances in Flame Retardant Chemistry and Science.* American Chemical Society, 251–270. doi:10.1021/bk-2012-1118.ch018

Papa, A. J., and Proops, W. R. (1972). Influence of Structural Effects of Halogen and Phosphorus Polyol Mixtures on Flame Retardancy of Flexible Polyurethane Foams. *J. Appl. Polym. Sci.* 16, 2361–2373. doi:10.1002/app.1972.070160915

Radhakrishnan, B., Ranjan, R., and Brittain, W. J. (2006). Surface Initiated Polymerizations from Silica Nanoparticles. *Soft Matter* 2, 386–396. doi:10.1039/B516508C

Salthammer, T., Fuhrmann, F., and Uhde, E. (2003). Flame Retardants in the Indoor Environment - Part II: Release of VOCs (Triethylphosphate and Halogenated Degradation Products) from Polyurethane. *Indoor Air* 13, 49–52. doi:10.1034/j.1600-0668.2003.01150.x

Singh, H., and Jain, A. K. (2008). Ignition, Combustion, Toxicity, and Fire Retardancy of Polyurethane Foams: a Comprehensive Review. *J. Appl. Polym. Sci.* 111, NA. doi:10.1002/app.29131

Sykam, K., Meka, K. K. R., and Donempudi, S. (2019). Intumescent Phosphorus and Triazole-Based Flame-Retardant Polyurethane Foams from castor Oil. *acs omega* 4, 1086–1094. doi:10.1021/acsomega.8b02968

Tsubokawa, N. (2007). Surface Grafting of Polymers onto Nanoparticles in a Solvent-free Dry-System and Applications of Polymer-Grafted Nanoparticles as Novel Functional Hybrid Materials. *Polym. J.* 39, 983–1000. doi:10.1295/polymj.PJ2007035

Vejayakumaran, P., Rahman, I. A., Sipaut, C. S., Ismail, J., and Chee, C. K. (2008). Structural and thermal Characterizations of Silica Nanoparticles Grafted with Pendant Maleimide and Epoxide Groups. *J. Colloid Interf. Sci.* 328, 81–91. doi:10.1016/j.jcis.2008.08.054

Wang, X., Song, L., Xing, W., Lu, H., and Hu, Y. (2011). A Effective Flame Retardant for Epoxy Resins Based on Poly(DOPO Substituted Dihydroxyl Phenyl Pentaerythritol Diphosphonate). *Mater. Chem. Phys.* 125, 536–541. doi:10.1016/j.matchemphys.2010.10.020

Wei, Y.-X., Deng, C., Zhao, Z.-Y., and Wang, Y.-Z. (2018). A Novel Organic-Inorganic Hybrid SiO2@DPP for the Fire Retardance of Polycarbonate. *Polym. Degrad. Stab.* 154, 177–185. doi:10.1016/j.polymdegradstab.2018.05.014

Xi, W., Qian, L., Huang, Z., Cao, Y., and Li, L. (2016). Continuous Flame-Retardant Actions of Two Phosphate Esters with Expandable Graphite in Rigid Polyurethane Foams. *Polym. Degrad. Stab.* 130, 97–102. doi:10.1016/j.polymdegradstab.2016.06.003

Xia, L., Liu, J., Li, Z., Wang, X., Wang, P., Wang, D., et al. (2020). Synthesis and Flame Retardant Properties of New boron-containing Polyurethane. *J. Macromolecular Sci. A* 57, 560–568. doi:10.1080/10601325.2020.1737543

Xie, F., Zhang, T., Bryant, P., Kurusingal, V., Colwell, J. M., and Laycock, B. (2019). Degradation and Stabilization of Polyurethane Elastomers. *Prog. Polym. Sci.* 90, 211–268. doi:10.1016/j.progpolymsci.2018.12.003

Xie, M., Zhang, S., Ding, Y., Wang, F., Liu, P., Tang, H., et al. (2017). Synthesis of a Heat-Resistant DOPO Derivative and its Application as Flame-Retardant in Engineering Plastics. *J. Appl. Polym. Sci.* 134, 44892–44903. doi:10.1002/app.44892

Xu, W., Wang, G., and Zheng, X. (2015). Research on Highly Flame-Retardant Rigid PU Foams by Combination of Nanostructured Additives and Phosphorus Flame Retardants. *Polym. Degrad. Stab.* 111, 142–150. doi:10.1016/j.polymdegradstab.2014.11.008

Xue, Y., Feng, J., Huo, S., Song, P., Yu, B., Liu, L., et al. (2020). Polyphosphoramide-intercalated MXene for Simultaneously Enhancing thermal Stability, Flame Retardancy and Mechanical Properties of Polylactide. *Chem. Eng. J.* 397, 125336. doi:10.1016/j.cej.2020.125336

Yang, H., Yu, B., Song, P., Maluk, C., and Wang, H. (2019). Surface-coating Engineering for Flame Retardant Flexible Polyurethane Foams: A Critical Review. *Composites Part B: Eng.* 176, 107185. doi:10.1016/j.compositesb.2019.107185

Yu, B., Yuen, A. C. Y., Xu, X., Zhang, Z.-C., Yang, W., Lu, H., et al. (2021). Engineering MXene Surface with POSS for Reducing Fire Hazards of Polystyrene with Enhanced thermal Stability. *J. Hazard. Mater.* 401, 123342. doi:10.1016/j.jhazmat.2020.123342

Yu, Z.-L., Yang, N., Apostolopoulou-Kalkavoura, V., Qin, B., Ma, Z.-Y., Xing, W.-Y., et al. (2018). Fire-retardant and Thermally Insulating Phenolic-Silica Aerogels. *Angew. Chem. Int. Ed.* 57, 4538–4542. doi:10.1002/anie.201711717

Yuan, B., Zhang, J., Yu, J., Song, R., Mi, Q., He, J., et al. (2016). Transparent and Flame Retardant Cellulose/aluminum Hydroxide Nanocomposite Aerogels. *Sci. China Chem.* 59, 1335–1341. doi:10.1007/s11426-016-0188-0

Zhang, Y., Jing, J., Liu, T., Xi, L., Sai, T., Ran, S., et al. (2021). A Molecularly Engineered Bioderived Polyphosphate for Enhanced Flame Retardant, UV-Blocking and Mechanical Properties of Poly(lactic Acid). *Chem. Eng. J.* 411, 128493. doi:10.1016/j.cej.2021.128493

Zhao, Y., Milanova, M., Warmoeskerken, M. M. C. G., and Dutschk, V. (2012). Surface Modification of TiO2 Nanoparticles with Silane Coupling Agents. *Colloids Surf. A: Physicochemical Eng. Aspects* 413, 273–279. doi:10.1016/j.colsurfa.2011.11.033

Zhi, M., Liu, Q., Zhao, Y., Gao, S., Zhang, Z., and He, Y. (2020). Novel MoS2-DOPO Hybrid for Effective Enhancements on Flame Retardancy and Smoke Suppression of Flexible Polyurethane Foams. *ACS omega* 5, 2734–2746. doi:10.1021/acsomega.9b03346

Zhu, H., Peng, Z., Chen, Y., Li, G., Wang, L., Tang, Y., et al. (2014). Preparation and Characterization of Flame Retardant Polyurethane Foams Containing Phosphorus-Nitrogen-Functionalized Lignin. *RSC Adv.* 4, 55271–55279. doi:10.1039/C4RA08429B